

Diamond growth in a high temperature and high pressure Fe-Ni-C-Si system: Effect of synthesis pressure

Yang Liu(刘杨), Zhiwen Wang(王志文), Bowei Li(李博维), Hongyu Zhao(赵洪宇), Shengxue Wang(王胜学), Liangchao Chen(陈良超), Hongan Ma(马红安), and Xiaopeng Jia(贾晓鹏)
Citation: Chin. Phys. B, 2023, 32 (**12**): 128102. DOI: 10.1088/1674-1056/acf03d
Journal homepage: http://cpb.iphy.ac.cn; http://iopscience.iop.org/cpb

What follows is a list of articles you may be interested in

Effects of oxygen/nitrogen co-incorporation on regulation of growth and properties of boron-doped diamond films

Dong-Yang Liu(刘东阳), Kun Tang(汤琨), Shun-Ming Zhu(朱顺明), Rong Zhang(张荣), You-Dou Zheng(郑有炓), and Shu-Lin Gu(顾书林)
Chin. Phys. B, 2023, 32 (**11**): 118102. DOI: 10.1088/1674-1056/ace4b7

Suppression and compensation effect of oxygen on the behavior of heavily boron-doped diamond films

Li-Cai Hao(郝礼才), Zi-Ang Chen(陈子昂), Dong-Yang Liu(刘东阳), Wei-Kang Zhao(赵伟康),Ming Zhang(张鸣), Kun Tang(汤琨), Shun-Ming Zhu(朱顺明), Jian-Dong Ye(叶建东),Rong Zhang(张荣), You-Dou Zheng(郑有炓), and Shu-Lin Gu(顾书林)
Chin. Phys. B, 2023, 32 (**3**): 038101. DOI: 10.1088/1674-1056/ac7f8a

Influence of the lattice parameter of the AlN buffer layer on the stress state of GaN film grown on (111) Si

Zhen-Zhuo Zhang(张臻琢), Jing Yang(杨静), De-Gang Zhao(赵德刚), Feng Liang(梁锋), Ping Chen(陈平), and Zong-Shun Liu(刘宗顺)
Chin. Phys. B, 2023, 32 (**2**): 028101. DOI: 10.1088/1674-1056/ac6b2b

Effect of oxygen on regulation of properties of moderately boron-doped diamond films

Dong-Yang Liu(刘东阳), Li-Cai Hao(郝礼才), Wei-Kang Zhao(赵伟康), Zi-Ang Chen(陈子昂), Kun Tang(汤琨), Shun-Ming Zhu(朱顺明), Jian-Dong Ye(叶建东), Rong Zhang(张荣), You-Dou Zheng(郑有炓), and Shu-Lin Gu(顾书林)
Chin. Phys. B, 2022, 31 (**12**): 128104. DOI: 10.1088/1674-1056/ac8e96

Effects of microwave oxygen plasma treatments on microstructure and Ge-V photoluminescent properties of diamond particles

Ling-Xiao Sheng(盛凌霄), Cheng-Ke Chen(陈成克), Mei-Yan Jiang(蒋梅燕), Xiao Li(李晓), Xiao-Jun Hu(胡晓君)
Chin. Phys. B, 2020, 29 (**8**): 088101. DOI: 10.1088/1674-1056/ab8db0

Diamond growth in a high temperature and high pressure Fe–Ni–C–Si system: Effect of synthesis pressure

Yang Liu(刘杨)[1], Zhiwen Wang(王志文)[1], Bowei Li(李博维)[1], Hongyu Zhao(赵洪宇)[1], Shengxue Wang(王胜学)[1], Liangchao Chen(陈良超)[2,§], Hongan Ma(马红安)[1,†], and Xiaopeng Jia(贾晓鹏)[1,‡]

[1] *State Key Laboratory of Superhard Materials, College of Physics, Jilin University, Changchun* 130012, *China*

[2] *Key Laboratory of Material Physics of Ministry of Education, School of Physics and Microelectronics, Zhengzhou University, Zhengzhou* 450052, *China*

(Received 18 June 2023; revised manuscript received 7 August 2023; accepted manuscript online 15 August 2023)

Pressure is one of the necessary conditions for diamond growth. Exploring the influence of pressure on growth changes in silicon-doped diamonds is of great value for the production of high-quality diamonds. This work reports the morphology, impurity content and crystal quality characteristics of silicon-doped diamond crystals synthesized under different pressures. Fourier transform infrared spectroscopy shows that with the increase of pressure, the nitrogen content in the C- center inside the diamond crystal decreases. X-ray photoelectron spectroscopy test results show the presence of silicon in the diamond crystals synthesized by adding silicon powder. Raman spectroscopy data shows that the increase in pressure in the Fe–Ni–C–Si system shifts the Raman peak of diamonds from 1331.18 cm^{-1} to 1331.25 cm^{-1}, resulting in a decrease in internal stress in the crystal. The half-peak width decreased from 5.41 cm^{-1} to 5.26 cm^{-1}, and the crystallinity of the silicon-doped diamond crystals improved, resulting in improved quality. This work provides valuable data that can provide a reference for the synthesis of high-quality silicon-doped diamonds.

Keywords: silicon-doped diamond, crystal quality, pressure effect, nitrogen content

PACS: 81.05.ug, 61.50.–f, 81.40.Vw, 91.62.La **DOI:** 10.1088/1674-1056/acf03d

1. Introduction

The establishment of mantle depth mineralogy is an important part of solid earth science and mantle dynamics. According to the available literature, the growth pressures for natural diamonds range from 5.5 GPa to 8.0 GPa, and the growth temperatures range from 1000 °C to 1400 °C.[1,2] Formed between 2.4 billion and 3.3 billion years ago, diamonds serve as important tools for exploring the mineral composition of the Earth's solid interior. They offer a unique way to obtain the deepest complete material from within the Earth.[3]

The Earth is not a uniform sphere, and there are differences in the proportion of material elements at different depths and positions.[4] Each material element in a natural diamond-formation environment underground will have an impact on the growth and nucleation of diamonds causing significant differences between diamond inclusions. For example, Han *et al.* explored crystal morphology as well as inclusion content at different temperatures.[5] With respect to the manufacture of synthetic diamonds, some inclusions have been used as raw materials in the manufacturing process.[6–8] Researchers have experimentally established different diamond growth models using the main elements of the inclusions.[9–12] By adjusting the pressure in the different models used to synthesize synthetic diamonds in order to simulate the growth of natural diamonds in the mantle, researchers can speculate on the depth of the growth environment of natural diamonds.[13] This can provide a valuable reference for determining the growth mechanism of natural diamonds and hence determining potential substances at different depths in the Earth's mantle.

The complete sp^3 structure diamond has many extraordinary characteristics and has fascinating applications in various fields.[14] Applications of diamonds are concentrated in three main areas, jewelry, mechanical engineering and electronics. In relation to jewelry, gemmologists are particularly interested in the origin, crystal growth and color of natural diamonds. For example, Qin *et al.* explored the effect of crystal seed size on the growth of single diamond crystals.[15] Wang *et al.* experimentally realized the shape-limited growth of large single type Ib diamond crystals.[16] The problem of cracked crystals can also be suppressed to a large extent by using a slow cooling process.[17] Guo *et al.* explored the synthesis of single type IIa diamond crystals by using Ti/Cu as a nitrogen absorber.[18] In mechanical engineering, the hardness and toughness of diamonds have been harnessed to make significant advancements in industrial processes. In the field of electronics, the thermal and semiconductor properties of diamonds have important value. The BN crystal form with graphite-diamond hybrid structure has excellent mechanical properties, as well as high ductility and hardness characteristics.[19] The electrical conductivity of boron and sulfur synergistically doped diamonds under high temperature and pressure has been reported.[20] The regulation of the growth quality and wetting performance of polycrystalline diamond films provides a reference for the

†Corresponding author. E-mail: maha@jlu.edu.cn
‡Corresponding author. E-mail: jiaxp@jlu.edu.cn
§Corresponding author. E-mail: chenlc@zzu.edu.cn

© 2023 Chinese Physical Society and IOP Publishing Ltd

practical application of diamond-based devices.[21] Currently, the color centers in diamonds play a significant role in the field of quantum communication. Cai *et al.* proved that regulation of the N–H–O impurity levels within the synthesis system can control the type of defect centers present in diamond crystals.[22] Sheng *et al.* expanded Ge–V diamond applications by finding methods to improve the luminescence performance of Ge–V color centers.[23] Si–V centers in diamonds are considered as possible single-photon sources. However, the creation of single-photon emitters has strict requirements in terms of the quality of the diamond crystal structure. Diamond structure quality can be estimated based on the width of Raman scattered light of 1332.00 cm^{-1}, as the presence of defects can lead to asymmetric widening of this line.[24] In addition, oxygen-related Si–V defects can preferentially improve the material properties of synthetic diamonds.[25] Increasing pressure reduces the effect of dopants on catalyst poisoning, which contributes to the growth of high-quality diamond single crystals. This provides ideas for the improved synthesis of high-quality silicon-doped diamonds.

In this study an Fe–Ni alloy is selected as the catalyst used to synthesize silicon-doped diamonds. The effects of pressure changes on the crystallization process, impurity content and crystal quality of silicon-doped diamond in Fe–Ni–C and Fe–Ni–C–Si systems are then investigated. It is hoped that the results from this study will provide improved information to support researchers exploring the quality and N content of diamonds at different depths in the Earth's mantle.

2. Experimental details

This study used a domestically produced large-capacity cubic high-pressure device (SPD-6 × 1200) to conduct high-pressure and high-temperature (HPHT) synthesis experiments on diamond crystals. The pressure range used was 5.8 GPa–6.8 GPa. The temperature range was 1600 K–1700 K. A schematic diagram of the HPHT equipment and the experimental device used for synthesizing diamonds is shown in Fig. 1. A {111} high-quality industrial grade diamond with a size of 1 mm was selected as the seed growth surface, along with high-purity flake graphite (purity of 99.99 wt.%) as the carbon source, Fe/Ni (80/20, mass ratio) as the catalyst solvent and Si powder (purity of 99.99 wt.%) as the additive. The high-purity graphite powder and Si powder were mixed evenly by weight in a mixer, and then pressed into a columnar carbon source for storage and backup. Variations in the quality and properties of the synthesized diamonds were investigated by regulating the pressure during synthesis. The pressure of the diamond synthesis experiment was calibrated using an oil pressure calibration curve established using the pressure inside the synthesis chamber and the high-pressure phase transition points of Bi, Tl and Ba. The temperature inside the chamber was estimated based on a relationship between input power and temperature measured by Pt 30% Rh/Pt 6% thermocouples. The measurement errors of both pressure and temperature in the synthesis system were each less than 1%.[6,26,27]

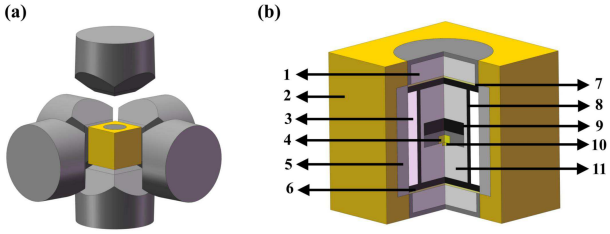


Fig. 1. Schematic diagram of the experimental system used to synthesize diamond in an HPHT environment: (a) an alloy hammer and sample cell; (b) schematic of the diamond growth cell: (1) steel cap; (2) pyrophyllite container; (3) dolomite container; (4) diamond sample; (5) NaCl + ZrO_2 sleeve; (6) graphite sheet; (7) Cu sheet; (8) graphite heater; (9) carbon source; (10) seed crystal; (11) ZrO_2 + MgO pillar.

At the end of the HPHT synthesis experiment, the samples were placed in a mixed solution of concentrated H_2SO_4 and concentrated HNO_3 (3:1 by volume) and boiled, with the aim of removing metal catalysts and graphite impurities from the crystal surface. Before testing, the synthesized diamond sample was placed in anhydrous ethanol for ultrasonic cleaning to remove small adsorbents from the crystal surface. The crystal morphology was observed using optical and scanning electron microscopy, and crystal photographs were taken under the same exposure conditions. The crystal in this study mainly exhibited a {111} crystal plane, so a VERTE 70 V Fourier transform microscopic infrared (FTIR) spectrometer was used to measure the infrared spectrum on the {111} crystal plane. The spectral resolution was greater than 0.4 cm^{-1} and the data collection range was 800 cm^{-1}–4000 cm^{-1}. The Renishaw inVia Raman spectrometer was used to measure the Raman spectrum of the crystal's {111} plane. The peak position error was controlled within 0.1 cm^{-1} and the spectral resolution was 1 cm^{-1}.

3. Results and discussion

3.1. Diamond growth morphology

In order to investigate the effect of pressure on the morphology of diamond growth, this experiment regulated the pressure used to synthesize diamond crystals and then analyzed and characterized the resulting crystals. Figure 2 presents an optical photo of a synthesized diamond from the Fe–Ni–C and the Fe–Ni–C–Si synthesis systems. Table 1 summarizes information such as pressure and temperature conditions and Si additive content in the carbon source and crystal.

Figures 2(a)–2(f) correspond to samples D-1–D-6 in Table 1, respectively. The experimental results show that all crystals had hexagonal octahedra with {111} crystal planes. In both synthesis systems, increased pressure caused the color of the synthesized crystals to gradually become lighter. Free N atoms inside a type Ib diamond can affect the color of the

crystal. When the color inside the crystal gradually changes from dark green to green, light green, yellow and light yellow, this indicates that the content of free N in the crystal has gradually decreased.[28] Estimated values of N content of the synthesized crystals are summarized in Table 1, and these results were also confirmed by subsequent FTIR characterization.

Table 1. Details of the experimental parameters used to synthesize diamond crystals in the Fe–Ni–C and the Fe–Ni–C–Si synthesis systems.

Run	Pressure (GPa)	Temperature (K)	Si (wt.%)	Growth time (h)	Growth face	Color	N content (ppm)
D-1	5.8	1600	0	12	{111}	yellow	279
D-2	6.3	1600	0	12	{111}	yellow	254
D-3	6.8	1600	0	12	{111}	yellow	241
D-4	5.8	1700	10	12	{111}	light yellow	68
D-5	6.3	1700	10	12	{111}	light yellow	59
D-6	6.8	1700	10	12	{111}	light yellow	51

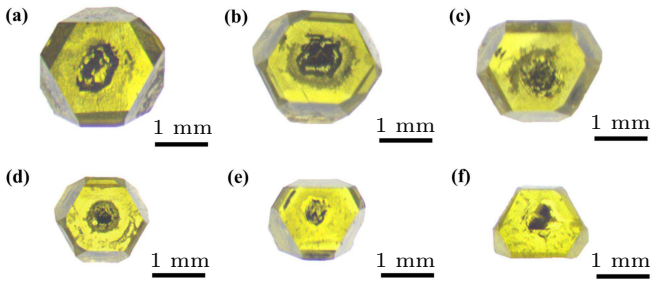


Fig. 2. Optical photos of diamond crystals synthesized in different experimental synthesis systems: (a) D-1; (b) D-2; (c) D-3; (d) D-4; (e) D-5; (f) D-6. See Table 1 for all associated experimental parameters.

In order to better observe and analyze the morphological characteristics of the synthesized diamond crystals under the different synthesis systems and pressures, scanning electron microscopy was used (Fig. 3). Under traditional HPHT diamond synthesis conditions (i.e., D-1), the diamond was not hindered or interfered with during the growth process. With the increase of pressure, the crystal surface gradually became complete and smooth, and high-quality crystals were synthesized. When Si powder was doped into the synthesis system (i.e., D-4), the crystal surface tended to be incomplete and the growth layer became rough. At the same time, a stepped morphology of the crystal surface was observed, with a large number of flaky defects appearing, but all these flaky defects were uniformly oriented in the same direction. This is due to a step-like growth trace left by the high-concentration doped diamond during the growth process, resulting in poor diamond crystal quality. The experiments show that when Si impurities are doped during the crystal synthesis process, Si and C in the lattice combine to form Si–C bonds, changing the length of C–C bonds and damaging the sp^3 diamond structure. This will hinder the normal epitaxial growth of the crystal plane, causing defects such as step-growth layers to form on the {111} plane, changing the growth characteristics of the diamond crystals, and ultimately preventing the growth and development of intact diamonds. However, there are many factors that can lead to changes in crystal morphology and further research is needed to clarify their mechanisms. At the same time, it can be observed from the results presented here that when the pressure increased from 5.8 GPa (D-4) to 6.8 GPa (D-6), the growth texture and defects on the crystal surface were significantly reduced, the growth layer gradually became smooth and the surface roughness of the crystal was greatly reduced. Hence the experiments demonstrate that increasing pressure can have a positive effect on the quality of silicon-doped synthetic diamonds.

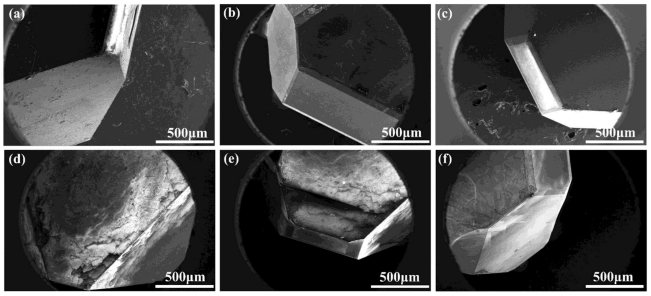


Fig. 3. Scanning electron microscopy images of diamond crystals synthesized under different pressures in different synthesis systems: (a) D-1; (b) D-2; (c) D-3; (d) D-4; (e) D-5; (f) D-6. See Table 1 for all associated experimental parameters.

3.2. FTIR characterization

Infrared spectroscopy plays a crucial role in the identification and analysis of diamond crystals, effectively identifying the types of defects and impurity elements inside diamonds, such as N, H, B, etc. Infrared spectroscopy can determine the form and content of N present inside diamond crystal. In the infrared spectrum, 1970 cm^{-1}, 2030 cm^{-1} and 2160 cm^{-1} are the characteristic peaks of diamond, representing the absorption peaks of the C–C bonds.[29] In addition, 1130 cm^{-1} and 1344 cm^{-1} correspond to the characteristic peaks of C-center N in the monophonon region,[30] and the peak absorption intensity represents the C-center N content in diamonds. In order to understand the effect of pressure on N content in crystals, this study obtained infrared absorption spectra of diamond samples at room temperature (Fig. 4). It can be seen that when the pressure was increased from 5.8 GPa to 6.8 GPa in the different synthesis systems, the absorption intensities of the 1130 cm^{-1} and 1344 cm^{-1} peaks tended to decrease.

The following equations were used to describe the con-

centration of N impurities in the synthesized diamond crystals:

$$N_{\mathrm{C}}\ (\mathrm{ppm}) = \frac{\mu\left(1130\ \mathrm{cm}^{-1}\right)}{\mu\left(2120\ \mathrm{cm}^{-1}\right)} \times 5.5 \times 25,$$

$$\mu\left(1130\ \mathrm{cm}^{-1}\right) = \left[A\left(1290\ \mathrm{cm}^{-1}\right) - A\left(1370\ \mathrm{cm}^{-1}\right)\right]/0.31,$$

$$\mu\left(2120\ \mathrm{cm}^{-1}\right) = \left[\frac{\left[40 \cdot A\left(2030\ \mathrm{cm}^{-1}\right) + 87 \cdot A\left(2160\ \mathrm{cm}^{-1}\right)\right]}{127} - A\left(2120\ \mathrm{cm}^{-1}\right)\right],$$

where N_{C} (ppm) represents the N concentration at the C-center inside a crystal and μ and A represent the correction coefficient and the absorption intensity, respectively.[31–33] The nitrogen concentration content of the diamond crystals synthesized under different synthesis systems was calculated using the above equations. The results are summarized in Table 1. In the Fe–Ni–C system, as the pressure increased from 5.8 GPa (D-1) to 6.8 GPa (D-3), the N content in the synthesized diamond decreased from 279 ppm to 241 ppm. In the Fe–Ni–C–Si system, the N content inside the silicon-doped diamond lattice decreased from 68 ppm (D-4) to 51 ppm (D-6). When the synthesis pressure increased, the N content in the diamond crystal decreased.

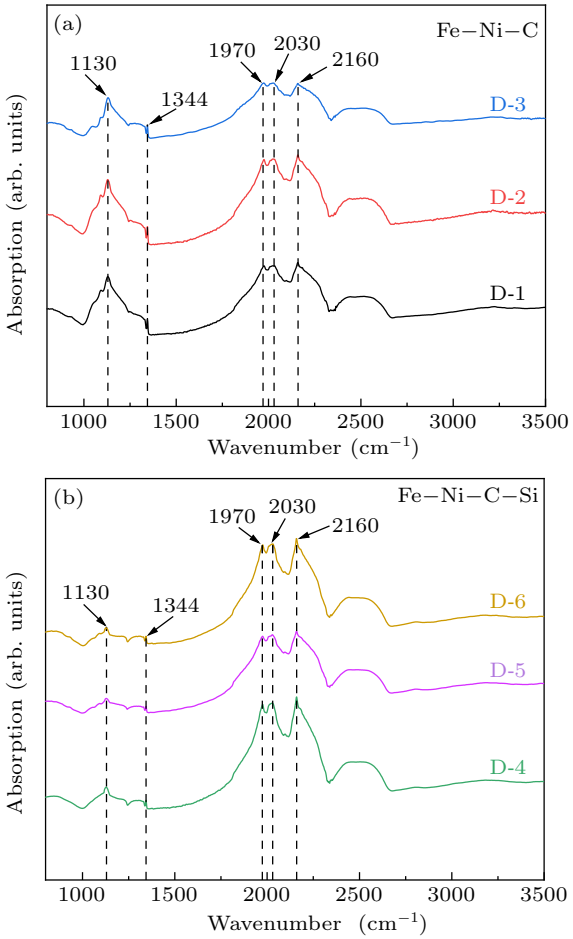


Fig. 4. FTIR spectra of diamond crystals synthesized under different pressures in different synthesis systems. See Table 1 for all associated experimental parameters.

Hence, the experimental results show that an increase in pressure can inhibit the entry of N into synthesized diamond crystal. Changes in pressure can have an impact on the performance of a catalyst in a synthesis system. Increasing pressure can increase the interaction between FeNi alloy and N atoms, thereby reducing the content of N atoms entering the lattice and directly affecting the N content inside diamond.[27,34] In addition, during HPHT experiments, doping is one of the methods that may be used to change the N content in diamonds. Si and N elements enter the diamond lattice together, forming Si–N bonds, resulting in a decrease in the N content of the lattice, and this was confirmed by the x-ray photoelectron spectroscopy (XPS) characterization. In summary, the influence of pressure on the N content of synthetic diamonds is caused by multiple factors and needs further exploration.

3.3. XRD characterization

In this experiment, a typical synthesized carbon source block (D-6. 10.0 wt.% Si) was characterized using an x-ray diffractometer, and the phase composition characteristics of the Fe–Ni–C–Si system were obtained, as shown in Fig. 5. In addition to diamond, graphite, Fe/Ni alloys and iron carbide, which are common in the metal–C system, SiC (PDF 04-0756), SiO_2 (PDF 82-1410) and Si_3N_4 (PDF 33-1160) are present in the carbon source block. The nitrogen content in the synthesized system is relatively certain, and there are two reasons why silicon doping reduces the nitrogen content of the diamond lattice. On the one hand, when the additive silicon reaches the low-temperature end of the crystal seed from the high-temperature end of the carbon source, the nitrogen atoms react with the Si in the molten Fe/Ni metal catalyst to form Si_3N_4, resulting in a decrease in the amount of nitrogen entering into the diamond. On the other hand, some of the nitrogen atoms enter into the diamond lattice in the form of bonding, and the bonding of N with Si leads to a decrease in the nitrogen content of the diamond lattice.

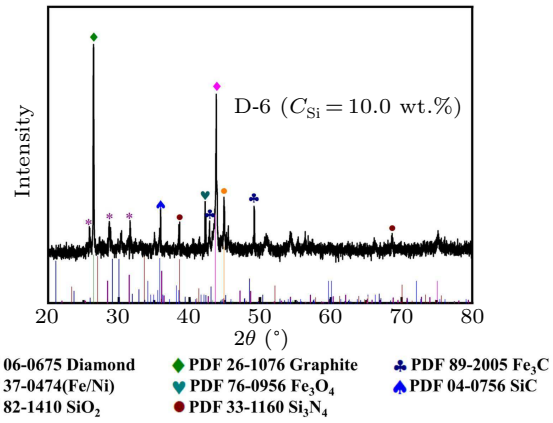


Fig. 5. XRD spectrum of 10.0 wt.% typical carbon source block (D-6) in the Fe–Ni–C–Si system.

3.4. XPS characterization

XPS can be used to characterize the chemical state, valence state, composition and relative content of atoms in diamond. This study used XPS to analyze the chemical states of C and Si atoms in experimentally synthesized diamond crystals. Figure 6 presents XPS spectra from the diamond crystal synthesized from a 10% Si source at 6.8 GPa pressure (D-6). After artificially crushing the sample, ultrasonic treatment was performed to remove impurities from the diamond surface and reduce experimental errors, and the analysis then aimed to characterize the crystal cross-section. Figures 6(a)–6(c) show the high-resolution XPS spectra of C 1s, N 1s and Si 2p, respectively. The four peaks obtained through peak-fitting in the high-resolution C 1s spectrum (Fig. 6(a)), correspond to sp^3–C, sp^2–C, C=O and C–Si bonds, respectively.[35] By fitting the resolution N 1s spectrum depicted in Fig. 5(b). the three peaks can be assigned to N–C, N–O and N–Si bonds (Fig. 6(b)).[36] The three peaks described in the high-resolution Si 2p spectrogram (Fig. 6(c)) correspond to Si–C, Si–N and Si–O bonds, respectively.[37] These results suggest that Si successfully entered the diamond lattice, and it can be seen that both Si and N atoms existed in the diamond. The bonding between Si and N in the lattice led to a decrease in N concentration.

3.5. Raman characterization

Raman spectroscopy can play a significant role in identifying C–C bond types in diamonds (such as graphite formed by sp^2 hybridization and diamond formed by sp^3 hybridization), as well as in natural diamond inclusions.[38] Raman spectroscopy curves can also reflect the internal structural changes of diamond crystals and distinguish the quality of diamond crystals. Raman spectroscopy has been widely used by researchers due to its non-destructive identification characteristics.[39] Figure 7(a) presents the Raman spectra of the diamonds synthesized under different synthesis systems and pressures, while figure 7(b) presents magnified images of the spectral data in the range of 1200.00 cm^{-1}–1500.00 cm^{-1}. The figure shows a strong and narrow characteristic peak in the Raman spectrum curve near 1332.00 cm^{-1}. Diamonds synthesized in different systems have high-quality sp^3 structures, without any sp^2 structures related to graphite (1580.00 cm^{-1}).[40] In order to better understand the shift of Raman peak positions, Gaussian fitting was performed on the data in this experiment. It was found that the Raman spectral peaks of Si-doped diamond crystals were straight without any excess peaks, but an increase in pressure would cause a slight shift in Raman peak positions.

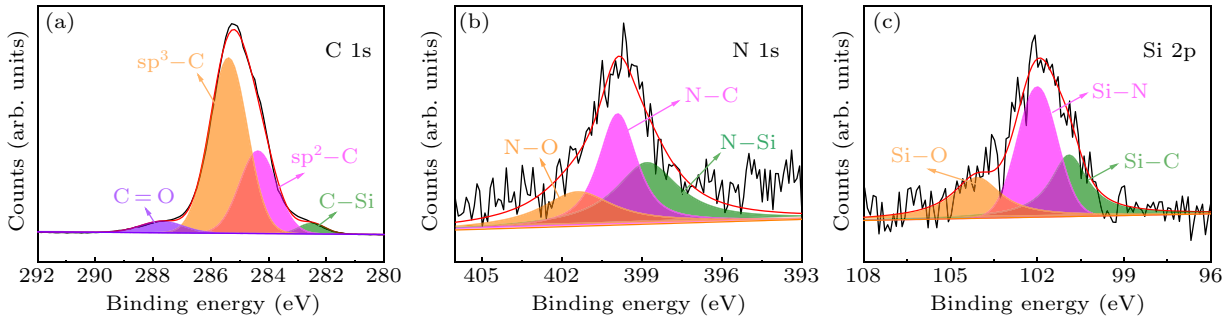


Fig. 6. The XPS spectra of a diamond crystal synthesized from a 10% Si source at 6.8 GPa pressure (D-6). (a) C 1s. (b) N 1s. (c) Si 2p.

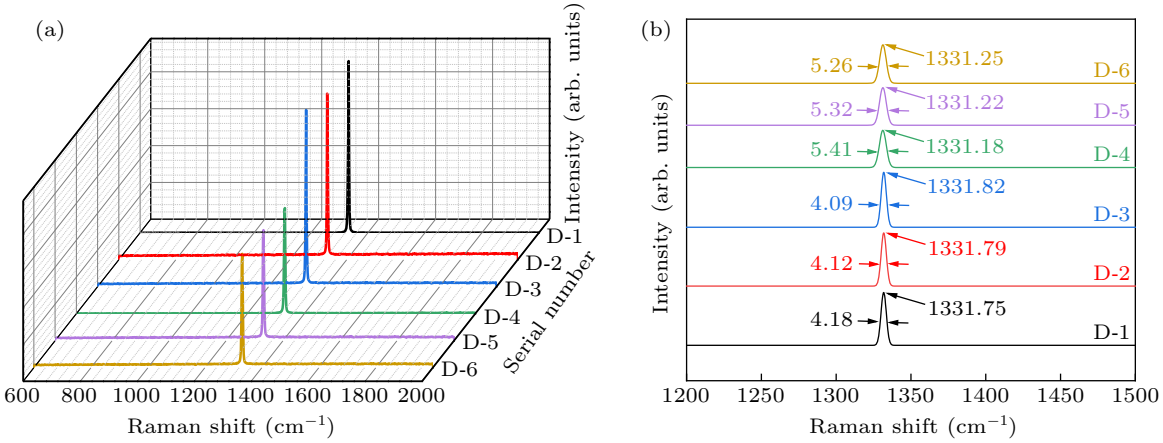


Fig. 7. (a) Raman spectra of diamond crystals synthesized under different pressures in different systems. (b) Magnified map of Raman spectral data within the range of 1200.00 cm^{-1}–1500.00 cm^{-1}. See Table 1 for all associated experimental parameters.

In order to observe the Raman peak position and halfwidth changes more clearly, figures 8(a) and 8(b) present the Raman peak position and halfwidth spectra of diamond crystals synthesized under different pressure conditions in the Fe–Ni–C (D-1–D-3) and Fe–Ni–C–Si (D-4–D-6) systems, respectively. When the FeNi catalytic system was not doped,

the effect of pressure on crystal quality was not significant. In the Fe–Ni–C–Si system, as the synthesis pressure increased, the Raman spectrum peak shifted from 1331.18 cm^{-1} to 1331.25 cm^{-1}, and the half-peak width decreased from 5.41 cm^{-1} to 5.26 cm^{-1}. Increasing the pressure in the doping system will reduce the internal stress of the crystal and increase the crystallinity of the diamond crystal. This suggests that with the increase of pressure, the quality of synthesized diamond crystals improves.

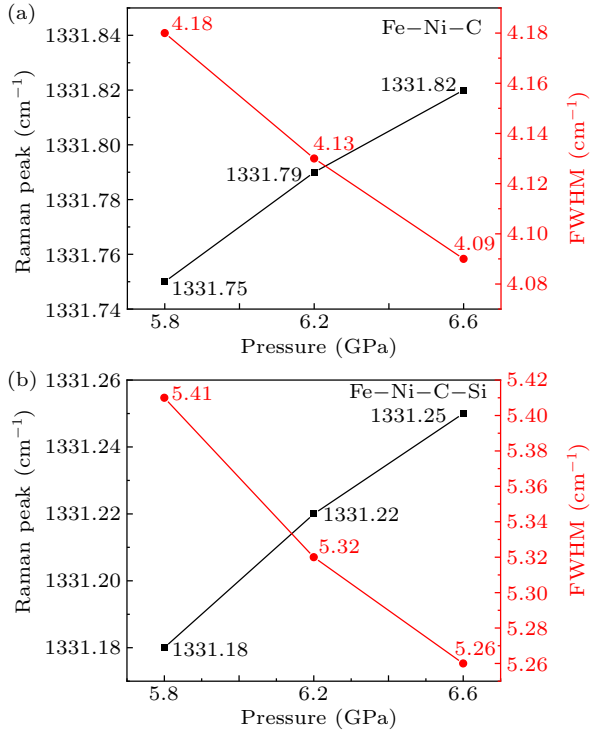


Fig. 8. Changes in Raman peak position and full-width at half-peak of synthesized diamond crystals under different pressure conditions. (a) Fe–Ni–C system. (b) Fe–Ni–C–Si system.

In order to calculate the surface residual stress of the diamond crystals synthesized in the Fe–Ni–C–Si system under different pressures, the following equation was used:[41]

$$\sigma_{\mathrm{h}}\ (\mathrm{GPa}) = \left[\gamma_0 - \gamma\ \left(\mathrm{cm}^{-1}\right)\right]/2.88.$$

Here, the calculated positive stress corresponds to the residual tensile stress on the crystal surface as shown in Table 2. As the pressure in the Fe–Ni–C–Si system increased from 5.8 GPa to 6.8 GPa, the residual tensile stress on the crystal surface also decreased from 0.28 GPa to 0.26 GPa. The residual stress on the surface of synthesized diamond is also influenced by the synthesis conditions. As the pressure increased, the residual stress gradually decreased and the crystal quality gradually improved.

Table 2. Raman shift and stress of diamond crystals synthesized under different pressure conditions in the Fe–Ni–C–Si system.

Run	Pressure (GPa)	Raman shift (cm^{-1})	$\Delta\gamma$ (cm^{-1})	Stress (GPa)
D-4	5.8	1331.18	0.82	0.28
D-5	6.3	1331.22	0.78	0.27
D-6	6.8	1331.25	0.75	0.26

3.6. Crystal growth process

Exploring the impact of pressure on diamond growth changes provides a valuable reference for understanding the growth mechanisms of different types of natural diamonds and the composition of materials at different mantle depths. The experiments reported here were used to construct a conceptual picture of diamond growth in the Fe–Ni–C–Si system under HPHT conditions (Fig. 9). When the pressure and temperature in the synthesis chamber resulted in the minimum diamond growth conditions, the temperature at the carbon source was higher than that at the diamond seed. The concentration difference of the different elements between the carbon source and the crystal seed position brought about by the temperature difference was the driving force for forming the diamond and other related products. At this point, the metal catalyst in the molten state served as the reaction site and transport channel for different elements. In the synthesis system, driven by the temperature difference, carbon elements passed through the FeNi catalyst from the carbon source and reached the surface of the seed crystal. The solubility of carbon in the low-temperature region will have resulted in deposition on the surface of the seed crystal in the form of diamond. With time, the silicon-doped diamond increased in size. The elements such as N, Si and O in the synthesis system also arrived at the diamond surface in a similar diffusion transport manner and entered the diamond crystal in the form of C–N, C–O, C–Si and N–Si bonds. The bonding between Si and N in the lattice led to a decrease in the N content of the diamond. At the same time, as the experimental synthesis pressure increased, the interaction between the FeNi metal solvent and N increased, and the number of N atoms dissolved in the FeNi metal catalyst increased, resulting in a decrease in the N content of the lattice. This conclusion was confirmed by the FTIR results. In addition, the decrease in the half-peak width of the Raman spectra also suggests that the increase in synthesis pressure in the system improved the quality of the diamond crystals.

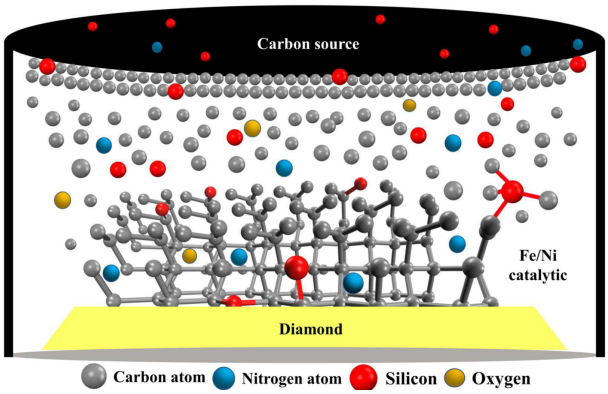


Fig. 9. Schematic diagram of the conceptual diamond crystal growth process as observed in the Fe–Ni–C–Si system.

4. Conclusion

In this study, diamond crystals were experimentally grown using an FeNi catalyst under different pressure conditions in Fe–Ni–C and Fe–Ni–C–Si systems, and the N content and quality changes of the resulting synthesized diamond crystals were studied. Diamond growth exhibited the characteristics of layered growth. When Si powder was added to the synthesis system, the crystal growth rate slowed down and the crystal color transitioned from yellow to light yellow. When the synthesis pressure increased, the crystal growth texture decreased and the surface roughness of the crystal decreased. In the Fe–Ni–C–Si synthesis system, the N content was relatively constant. When the synthesis pressure increased, if the N content in the crystal decreased, the N content in other media, such as in the metal solvents, increased. Infrared spectroscopy confirmed that the introduction of Si during the synthesis of diamond crystals reduced the N content in the C-center of the diamond, and the ability of the FeNi catalyst to dissolve N also changed with increasing pressure. A portion of the N atoms dissolved in the molten FeNi alloy, and the combined effect of the two led to a decrease in the N content of the diamond lattice. Raman spectral analysis results showed that, in the Fe–Ni–C–Si system, Si atoms entered the diamond lattice, increasing the internal stress of the crystal and causing defects in the crystal, affecting the crystallinity and quality of the diamond crystal. Increasing the pressure during the synthesis phase improved the quality of diamond crystals, which was confirmed by a decrease in the half-peak width of the Raman spectra.

In summary, pressure can affect the growth characteristics of diamonds. This provides insights for studying the properties of materials at different depths beneath the mantle and their ability to dissolve N. This article demonstrates methods to improve the quality of silicon-doped diamonds by increasing synthesis pressure, providing an effective reference for further exploration of silicon-doped diamonds and SiV color centers in the future.

Acknowledgment

Project supported by the National Natural Science Foundation of China (Grant Nos. 51872112 and 51772120).

References

[1] Pearson D G, Brenker F E, Nestola F, McNeill J, Nasdala L, Hutchison M T, Matveev S, Mather K, Silversmit G, Schmitz S, Vekemans B and Vincze L 2014 *Nature* **507** 221
[2] Bureau H, Frost D J, Bolfan-Casanova N, Leroy C, Esteve I and Cordier P 2016 *Lithos* **265** 4
[3] Nestola F, Korolev N, Kopylova M, Rotiroti N, Pearson D G, Pamato M G, Alvaro M, Peruzzo L, Gurney J J, Moore A E and Davidson J 2018 *Nature* **555** 237
[4] Mashino I, Miozzi F, Hirose K, Morard G and Sinmyo R 2019 *Earth and Planetary Science Letters* **515** 135
[5] Han F, Li S S, Jia X F, Chen W Q, Su T C, Hu M H, Yu K P, Wang J K, Wu Y M, Ma H A and Jia X P 2019 *Chin. Phys. B* **28** 028103
[6] Fang S, Ma H, Cai Z H, Wang C X, Fang C, Zhao Z D, Lu Z Y, Wang Y K, Chen L and Jia X 2020 *CrystEngComm* **22** 602
[7] Fang S, Ma H, Cai Z h, Wang C X, Fang C, Lu Z, Wang Y K, Chen L and Jia X 2020 *CrystEngComm* **22** 3854
[8] Kanda H, Akaishi M and Yamaoka S 1999 *Diam. Relat. Mater.* **8** 1441
[9] Fang C, Shen W, Zhang Y, Mu P, Zhang Z and Jia X 2019 *Crystal Growth & Design* **19** 3955
[10] Palyanov Y, Kupriyanov I, Borzdov Y, Nechaev D and Bataleva Y 2017 *Crystals* **7** 119
[11] Lu Z, Zhao H, Wang Y, Fang S, Cai Z, Wang Z, Ma H A, Chen L, Jia H and Jia X 2021 *Lithos* **404–405** 106470
[12] Cai Z, Li M, Chen L, Fang S, Wang Z, Zhao H, Ma H and Jia X 2022 *CrystEngComm* **24** 1773
[13] Fang S, Wang Y, Chen L, Lu Z, Cai Z, Fang C, Zhao Z, Ma H and Jia X 2021 *CrystEngComm* **23** 1406
[14] Lv R, Yang X, Yang D, Niu C, Zhao C, Qin J, Zang J, Dong F, Dong L and Shan C 2021 *Chin. Phys. Lett.* **38** 076101
[15] Qin Y K, Xiao H Y, Liu L N, Sun R R, Hu Q B, Bao Z G, Zhang Y S, Li S S and Jia X P 2019 *Acta Phys. Sin.* **68** 020701 (in Chinese)
[16] Wang J Z, Li S S, Su T C, Hu M H, Hu Q, Wu Y M, Wang J K, Han F, Yu K P, Gao G J, Guo M M, Jia X P, Ma H A and Xiao H Y 2018 *Acta Phys. Sin.* **67** 168101 (in Chinese)
[17] Xiao H Y, Qin Y K, Liu L N, Bao Z G, Tang C J, Sun R R, Zhang Y S, Li S S and Jia X P 2018 *Acta Phys. Sin.* **67** 140702 (in Chinese)
[18] Guo M M, Li S S, Hu M H, Su T C, Wang J Z, Gao G J, You Y and Nie Y 2020 *Chin. Phys. B* **29** 018101
[19] Luo K, Li B, Sun L, Wu Y, Ge Y, Liu B, He J, Xu B, Zhao Z and Tian Y 2022 *Chin. Phys. Lett.* **39** 036301
[20] Li Y, Wang Y, Li S S, Li Z B, Luo K W, Ran M W and Song M S 2019 *Acta Phys. Sin.* **68** 098101 (in Chinese)
[21] Wan L, Mu C, Liu X, Cheng S, Wang Q, Li L, Li H and Zhou G 2022 *Chin. Phys. Lett.* **39** 036801
[22] Cai Z, Li B, Chen L, Wang Z, Fang S, Wang Y, Ma H and Jia X 2022 *Chin. Phys. B* **31** 108104
[23] Sheng L X, Chen C K, Jiang M Y, Li X and Hu X J 2020 *Chin. Phys. B* **29** 088101
[24] Ekimov E A and Kondrin M V 2017 *Physics-Uspekhi* **60** 539
[25] Hu X J and Li N 2013 *Chin. Phys. Lett.* **30** 088102
[26] Guo L, Ma H, Chen L, Chen N, Miao X, Wang Y, Fang S, Yang Z, Fang C and Jia X 2018 *CrystEngComm* **20** 5457
[27] Chen N, Ma H, Chen L, Yan B, Fang C, Liu X, Li Y, Guo L, Chen L and Jia X 2018 *International Journal of Refractory Metals and Hard Materials* **71** 141
[28] Liang Z Z, Kanda H, Jia X, Ma H A, Zhu P W, Guan Q F and Zang C Y 2006 *Carbon* **44** 913
[29] Fallon P J, Brown L M, Barry J C and Bruley J 1995 *Philos. Mag. A* **72** 21
[30] Pal'Yanov N, Sokol A G, Borzdov M and Khokhryakov A F 2002 *Lithos* **60** 145
[31] Yu R Z, Ma H A, Liang Z Z, Liu W Q, Zheng Y J and Jia X 2008 *Diam. Relat. Mater.* **17** 180
[32] Ashfold M N R, Goss J P, Green B L, May P W, Newton M E and Peaker C V 2020 *Chem. Rev.* **120** 5745
[33] Yan B, Jia X, Fang C, Chen N, Li Y, Sun S and Ma H A 2016 *International Journal of Refractory Metals and Hard Materials* **54** 309
[34] Fang S, Ma H, Wang Z, Yang Z, Cai Z H, Ding L, Miao X, Chen L and Jia X 2019 *CrystEngComm* **21** 6010
[35] Ahmed M H, Byrne J A, Mclaughlin J and Ahmed W 2013 *J. Biomater. Nanobiotechnol.* **04** 194
[36] Mangeney C, Qin Z, Dahoumane S A, Adenier A, Herbst F, Boudou J P, Pinson J and Chehimi M M 2008 *Diam. Relat. Mater.* **17** 1881
[37] Ténégal F, Rocque A G d l, Dufour G, Sénémaud C, Doucey B, Bahloul-Hourlier D, Goursat P, Mayne M and Cauchetier M 2000 *J. Electron Spectrosc. Relat. Phenomena* **109** 241
[38] Wang Z Y, Dong L H, Wang D S and Dong Y H 2012 *Precis. Eng.* **36** 162
[39] Miao X, Chen L, Ma H, Fang C, Guo L, Wang Z, Yang Z, Zhao Z and Jia X 2019 *CrystEngComm* **21** 3961
[40] Wang J, Li S, Hu M, Su T and Nie Y 2020 *International Journal of Refractory Metals and Hard Materials* **87** 105150
[41] Catledge S A, Vohra Y K, Ladi R and Rai G 1996 *Diam. Relat. Mater.* **5** 1159